J|A|C|S
ARTICLES
Published on Web 07/07/2006

Silver Bromide Nanoparticle/Polymer Composites: Dual Action Tunable Antimicrobial Materials

Varun Sambhy, Megan M. MacBride, Blake R. Peterson, and Ayusman Sen*

Contribution from the Department of Chemistry, The Pennsylvania State University, University Park, Pennsylvania 16802

Received March 1, 2006; E-mail: asen@psu.edu

Abstract: We present a simple method of fabricating highly potent dual action antibacterial composites consisting of a cationic polymer matrix and embedded silver bromide nanoparticles. A simple and novel technique of on-site precipitation of AgBr was used to synthesize the polymer/nanoparticle composites. The synthesized composites have potent antibacterial activity toward both gram-positive and gram-negative bacteria. The materials form good coatings on surfaces and kill both airborne and waterborne bacteria. Surfaces coated with these composites resist biofilm formation. These composites are different from other silver-containing antibacterial materials both in the ease of synthesis and in the use of a silver salt nanoparticle instead of elemental silver or complex silver compounds. We also demonstrate the ability to tune the release of biocidal Ag^+ ions from these composites by controlling the size of the embedded AgBr nanoparticles. These composites are potentially useful as antimicrobial coatings in a wide variety of biomedical and general use applications.

1. Introduction

Antimicrobial modification of surfaces to prevent growth of detrimental microorganisms is a highly desired objective. Microbial adhesion to surfaces followed by cell growth and colonization results in the formation of a compact biofilm matrix capable of protecting the underlying microbes from antibiotics and host defense mechanisms.[1] In case of biomedical devices such as catheters, prosthetics, implants, and so forth, surface microbial infestation can result in serious infection and device failure.[2] Surface-centered infections are also implicated in food spoilage, spread of foodborne diseases, and biofouling of materials.[3] Hence, there is a significant interest in the development of antimicrobial materials and surfaces for applications in the health and biomedical device industry, food industry, and personal hygiene industry. Antimicrobial coatings need to combine desirable attributes such as potent antibacterial efficacy, environmental safety, low toxicity, and ease of fabrication.

Three broad classes of materials have been used for rendering surfaces antimicrobial: (a) contact active ampiphilic polymers,[4] or synthetic mimics of naturally occurring antibacterial peptides,[5] (b) microbe-repelling anti-adhesive polymers,[6] and (c) polymeric/composite materials loaded with slow releasing biocides such as heavy metals,[7] antibiotics,[8] small molecule biocides,[9] halogen species,[10] and nitric oxide.[11] Among the third class of antimicrobials, silver-based materials are of special interest. The

(1) (a) Costerton, W.; Stewart, P. S.; Greenberg, E. P. *Science* **1999**, *284*, 1318−1322. (b) O'Toole, G. A.; Stewart, P. S. *Nat. Biotechnol.* **2005**, *23*, 1378−1379. (c) Hoffman, L. R.; Lucas R.; D'Argenio, D. A.; MacCoss, M. J.; Zhang, Z.; Jones, R. A.; Miller, S. I. *Nature* **2005**, *436*, 1171−1175. (d) Mah, T. F.; Pitts, B.; Pellock, B.; Walker, G. C.; Stewart, P. S.; O'Toole, G. A. *Nature* **2003**, *426*, 306−310.

(2) (a) Barth, E.; Myrvik, Q. M.; Wagner, W.; Gristina, A. G. *Biomaterials* **1989**, *10*, 325−328. (b) Raad, I. I.; Hanna, H. A.; Boktour, M.; Chaiban, G.; Hachem, R. Y.; Dvorak, T.; Lewis, R.; Murray, B. E. *Antimicrob. Agents Chemother.* **2005**, *49*, 5046−5050. (c) Jones, G. L.; Muller, C. T.; O'Reilly, M.; Stickler, D. J. *J. Antimicrob. Chemother.* **2006**, *57*, 266−272. (d) Millsap, K. W.; Reid, G.; van der Mei, H. C.; Busscher, H. J. *Biomaterials* **1997**, *18*, 87−91. (e) Arciola, C. R.; Campoccia, D.; Gamberini, S.; Donati, M. E.; Pirini, V.; Visai, L.; Speziale, P.; Montanaro, L. *Biomaterials* **2005**, *26*, 6530−6535.

(3) (a) Nuzzo, R. G. *Nat. Mater.* **2003**, *2*, 207−208. (b) Greenberg, C. B.; Steffek, C. *Thin Solid Films* **2005**, *484*, 324−327.

(4) (a) Tashiro, T. *Macromol. Mater. Eng.* **2001**, *286*, 63−87. (b) Ilker, M. F.; Nüsslein, K.; Tew, G. N.; Coughlin, B. E. *J. Am. Chem. Soc.* **2004**, *126*, 15870−15875. (c) Kuroda, K.; DeGrado, W. F. *J. Am. Chem. Soc.* **2005**, *127*, 4128−4129. (d) Lee, S. B.; Koepsel, R. R.; Morley, S. W.; Matyjaszewski, K.; Sun, Y.; Russell, A. J. *Biomacromolecules* **2004**, *5*, 877−882. (e) Ilker, M. F.; Schule, H.; Coughlin, E. B. *Macromolecules* **2004**, *37*, 694−700. (f) Dizman, B.; Elasri, M. O.; Mathias, L. *J. Appl. Polym. Sci.* **2004**, *94*, 635−642. (g) Alasino, R. V.; Ausar, S. F.; Bianco, I. D.; Castagna, L. F.; Contigiani, M.; Beltramo, D. M. *Macromol. Biosci.* **2005**, *5*, 207−213.

(5) (a) Tang, H.; Doerksen, R. J.; Tew, G. N. *Chem. Commun.* **2005**, *12*, 1537−1539. (b) Tew, G. N.; Liu, D.; Chen, Bi.; Doerksen, R. J.; Kaplan, J.; Carroll, P. J.; Klein, M. L.; DeGrado, W. F. *Proc. Natl. Acad. Sci. U.S.A.* **2002**, *99*, 5110−5114. (c) Liu, D.; DeGrado W. F. *J. Am. Chem. Soc.* **2001**, *123*, 7553−7559.

(6) (a) Desai, N. P.; Hossainy, S. F.; Hubbell, J. A. *Biomaterials* **1992**, *12*, 417−420. (b) Ignatova, M.; Voccia, S.; Gilbert, B.; Markova, N.; Cossement, D.; Gouttebaron, R.; Jerome, R.; Jerome, C. *Langmuir* **2006**, *22*, 255−262. (c) Lin, J.; Murthy, S. K.; Olsen, B. D.; Gleason, K. K.; Klibanov, A. M. *Biotechnol. Lett.* **2003**, *25*, 1661−1665.

(7) (a) Ho, C. H.; Tobis, J.; Christina, S.; Thoman R.; Tiller, J. C. *Adv. Mater.* **2004**, *16*, 957−961. (b) Cioffi, N.; Torsi, L.; Ditaranto, N.; Tantillo, G.; Ghibelli, L.; Sabbatini, L.; Bleve-Zacheo, T.; D'Alessio, M.; Zambonin, P. G.; Traversa, E. *Chem. Mater.* **2005**, *17*, 5255−5262. (c) Weickmann, H.; Tiller, J. C.; Thomann, R.; Muelhaupt, R. *Macromol. Mater. Eng.* **2005**, *290*, 875−883. (d) Tsukada, M.; Arai, T.; Colonna, G. M.; Boschi, A.; Freddi, G. *J. Appl. Polym. Sci.* **2003**, *89*, 638−644. (e) McDonnell, A. M. P.; Beving, D.; Wang, A.; Chen, W.; Yan, Y. *Adv. Funct. Mater.* **2005**, *15*, 336−340.

(8) (a) Kohnen, W.; Kolbenschlag, C.; Keiser, S. T.; Jansen, B. *Biomaterials* **2003**, *24*, 4865−4869. (b) Maeyama, R.; Kwon, I. K.; Mizunoe, Y.; Anderson, J. M.; Tanaka, M.; Matsuda, T. *J. Biomed. Mater. Res.* **2005**, *75A*, 146−155. (c) Changez, M.; Koul, V.; Dinda, A. *Biomaterials* **2004**, *26*, 2095−2104. (d) Dizman, B.; Elasri, M. O.; Mathias, L. J. *Biomacromolecules* **2005**, *6*, 514−520.

(9) (a) Gerrard, J. J.; Annable, J. A.; Moore, J. *Surf. Coat. Int., Part B* **2005**, *88*, 83−91. (b) Iconomopoulou, S. M.; Voyiatzis, G. A. *J. Controlled Release* **2005**, *103*, 451−464.

10.1021/ja061442z CCC: $33.50

silver ion exhibits broad-spectrum biocidal activity toward many different bacteria, fungi, and viruses[12] and is believed to be the active component in silver-based antimicrobials. Ag^+ ion is known to deactivate cellular enzymes and DNA by coordinating to electron-donating groups such as thiols, carboxylates, amides, imidazoles, indoles, hydroxyls, and so forth.[13] Silver is also know to cause pits in bacterial cell walls, leading to increased permeability and cell death.[14] Silver has low toxicity toward mammalian cells[15] and does not easily provoke microbial resistance.[16] Hence, silver-containing materials have been widely used by the biomedical industry in catheters,[17] dental material,[18] medical devices and implants,[19] and wound and burn dressings.[20] Most of the techniques used to incorporate silver into polymeric matrixes involve either chemical workups such as reduction[21] or synthesis of complex silver compounds,[22] mixing preformed silver particles with polymers,[23] or complicated physical techniques[24] such as sputtering[25] and plasma deposition.[26] All these techniques add time, cost, and complexity to the overall process of fabrication of the antimicrobial material. Hence, a simpler method to incorporate silver into polymers is desirable.

Most silver-containing antimicrobial polymers consist of either elemental silver, which has a very low rate of dissolution in aqueous environment,[7a,17b,18,19b,21,23] or highly water-soluble silver salts or silver(I) complexes.[7e,19c,22a] Substitution by a sparingly soluble silver salt in place of elemental silver should significantly increase the rate of generation of biocidal Ag^+ ion over that from elemental silver, while limiting uncontrolled dissolution as would be the case for freely soluble silver species. In particular, silver halides have the potential to be antimicrobial by providing a constant concentration of biocidal Ag^+ ions in aqueous environments [K_{sp} (AgBr), 5×10^{-13}].[27] Additionally, it should be possible to tailor the rate of release of Ag^+ ion into the surrounding medium by appropriate choice of the encapsulating polymer and the size of the embedded silver halide particles.

In this article, we describe cationic polymer/silver bromide nanoparticle composites having potent long-lasting antibacterial activity toward both gram-positive and gram-negative bacteria. The two-component composites consist of a cationic polymer, poly(4-vinyl-*N*-hexylpyridinium bromide), and embedded silver bromide nanoparticles. Poly(4-vinyl-*N*-alkylpyridinium)-based polymers have been shown to have potent antibacterial activity toward both gram-positive and gram-negative bacteria due to their membrane-disrupting ability.[4a,28] At the same time, pyridinium polymers are nontoxic toward mammalian cells.[29] Silver bromide nanoparticles serve as a source of strongly biocidal but nontoxic Ag^+ ions.[15] The water-insoluble composites form good coatings on glass and exhibited long-lasting antibacterial properties toward both airborne and waterborne bacteria. A simple technique of on-site precipitation was used to synthesize the polymer/nanoparticle composites. This technique forms the composite from the starting materials in one-pot and significantly reduces the difficulties associated with forming organic−inorganic hybrids with embedded nanoparticles. We also demonstrate the ability to tune the antibacterial activity of these composites by controlling the size of the embedded AgBr nanoparticles.

2. Results and Discussion

2.1. Composite Synthesis and Characterization. The on-site precipitation technique is schematically depicted in Figure 1. The bromide anions associated with the polymer side chains of the ampiphilic pyridinium polymer **NPVP** were precipitated by the addition of a silver salt. The resulting silver bromide nanoparticles are stabilized by the capping and steric effect of the polymer. Although precipitation chemistry has been widely

(10) (a) Chen, Y.; Worley, S. D.; Kim, J.; Wei, C. I.; Chen, T. Y.; Santiago, J. I.; Williams, J. F.; Sun, G. *Ind. Eng. Chem. Res.* **2003**, *42*, 280−284. (b) Sun, Y.; Sun, G. *Macromolecules* **2002**, *35*, 8909−8912. (c) Sun, Y.; Sun, G. *Ind. Eng. Chem. Res.* **2004**, *43*, 5015−5020.

(11) (a) Nablo, B. J.; Chen, T. Y.; Schoenfisch, M. H. *J. Am. Chem. Soc.* **2001**, *123*, 9712−9713. (b) Nablo, B. J.; Rothrock, A. R.; Schoenfisch, M. H. *Biomaterials* **2004**, *26*, 917−924. (c) Robbins, M. E.; Hopper, E. D.; Schoenfisch, M. H. *Langmuir* **2004**, *20*, 10296−10302.

(12) (a) Russel, A. D.; Hugo, W. B. *Prog. Med. Chem.* **1994**, *31*, 351−370. (b) Zachariadis, C. P.; Hadjikakou, S. K.; Hadjiliadis, N.; Skoulika, S.; Michaelides, A.; Balzarini, J.; De Clercq, E. *Eur. J. Inorg. Chem.* **2004**, *7*, 1420−1426.

(13) (a) Feng, G. L.; Wu, J.; Chen, G. Q.; Cui, F. Z.; Kim, T. M.; Kim, J. O. *J. Biomed. Mater. Res.* **2000**, *52*, 662−668. (b) Holt, K. B.; Bard, A. J. *Biochemistry* **2005**, *44*, 13214−13223.

(14) Sondi, I.; Salopek-Sondi, B. *J. Colloid Interface Sci.* **2004**, *275*, 177−182.

(15) (a) Hollinger, M. A. *Crit. Rev. Toxicol.* **1996**, *26*, 255−260. (b) Gosheger, G.; Hardes, J.; Ahrens, H.; Streitburger, A.; Buerger, H.; Erren, M.; Gunsel, A.; Kemper, F. H.; Winkelmann, W.; von Eiff, C. *Biomaterials* **2004**, *25*, 5547−5556.

(16) (a) Percival, S. L.; Bowler, P. G.; Russell, D. *J. Hosp. Infect.* **2005**, *60*, 1−7. (b) Brady, M. J.; Lisay, C. M.; Yurkovetskiy, A. V.; Sawan, S. P. *Am. J. Infect. Control* **2003**, *31*, 208−214.

(17) (a) Rosato, A. E.; Tallent, S. M.; Edmond, M. B.; Bearman, G. M. *Am. J. Infect. Control* **2004**, *32*, 486−488. (b) Rupp, M. E.; Fitzgerald, T.; Marion, N.; Helget, V.; Puumala, S.; Anderson, J. R.; Fey, P. D. *Am. J. Infect. Control* **2004**, *32*, 445−450. (c) Hachem, R. Y.; Wright, K. C.; Zermeno, A.; Bodey, G. P.; Raad, I. I. *Biomaterials* **2003**, *24*, 3619−3622. (d) Oloffs, A.; Grosse-Siestrup, C.; Bisson, S.; Rinck, M.; Rudolph, R.; Gross, U. *Biomaterials* **1994**, *15*, 753−758.

(18) (a) Yoshida, K.; Tanagawa, M.; Atsuta, M *J. Biomed. Mater. Res.* **1999**, *47*, 516−522. (b) Morrier, J.-J.; Suchett-Kaye, G.; Nguyen, D.; Rocca, J.-P.; Blanc-Benon, J.; Barsotti, O. *Dent. Mater.* **1998**, *14*, 150−157. (c) Ueshige, M.; Abe, Y.; Sato, Y.; Tsuga, K.; Akagawa, Y.; Ishii, M. *J. Dent.* **1999**, *27*, 517−522.

(19) (a) Rupp, M. E.; Lisco, S. J.; Lipsett, P. A.; Perl, T. M.; Keating, K.; Civetta, J. M.; Mermel, L. A.; Lee, D.; Dellinger, P.; Donahoe, M.; Giles, D.; Pfaller, M. A.; Maki, D. G.; Sherertz, R. *Ann. Int. Med.* **2005**, *143*, 570−580. (b) Masse, A.; Bruno, A.; Bosetti, M.; Biasibetti, A.; Cannas, M.; Gallinaro, P. *J. Biomed. Mater. Res.* **2000**, *53*, 600−604. (c) Multanen, M.; Talja, M.; Hallanvuo, S.; Siitonen, A.; Valimaa, T.; Tammela, T. L. J.; Seppala, J.; Tormala, P. *Urol. Res.* **2000**, *28*, 327−331. (d) Multanen, M.; Talja, M.; Tammela, T. L. J.; Seppala, J.; Valimaa, T.; Jarvi, K.; Tormala, P. *Urol. Res.* **2001**, *29*, 113−117. (e) Davenas, J.; Thevenard, P.; Philippe, F.; Arnaud, M. N. *Biomol. Eng.* **2002**, *19*, 263−268.

(20) (a) Price, W. R,; Wood, M. *Am. J. Surg.* **1966**, *112*, 674−680. (b) Meaume, S.; Vallet, D.; Morere, M. N.; Teot, L. *J. Wound Care* **2005**, *14*, 411−419. (c) Kim, H. J.; Choi, E. Y.; Oh, J. S.; Lee, H. C.; Park, S. S.; Cho, C. S. *Biomaterials* **2000**, *21*, 131−141. (d) Parikh, D. V.; Fink, T.; Rajasekharan, K.; Sachinvala, N. D.; Sawhney, A. P. S.; Calamari, T. A.; Parikh, A. D. *Text. Res. J.* **2005**, *75*, 134−138.

(21) (a) Aymonier, C.; Schlotterbeck, U.; Antonietti, L.; Zacharias, P.; Thomann, R.; Tiller, J. C.; Mecking, S. *Chem. Commun.* **2002**, *24*, 3018−3019. (b) Joly, S.; Kane, R.; Radzilowski, L.; Wang, T. C.; Wu, A.; Cohen, R. E.; Thomas, E. L.; Rubner, M. F. *Langmuir* **2000**, *16*, 1354−1359. (c) Wang, X. S.; Wang, H.; Coombs, N.; Winnik, M. A.; Manners, I. *J. Am. Chem. Soc.* **2005**, *127*, 8924−8925. (d) Porel, S.; Singh, S.; Harsha, S. S.; Rao, D. N.; Radhakrishnan, T. P. *Chem. Mater.* **2005**, *17*, 9−12. (e) Chauhan, B. P. S.; Sardar, R. *Macromolecules* **2004**, *37*, 5136−5139.

(22) (a) Melaiye, A.; Sun, Z.; Hindi, K.; Milsted, A.; Ely, D.; Reneker, D.; Tessier, C. A.; Youngs, W. *J. Am. Chem. Soc.* **2005**, *127*, 2285−2291. (b) Kasuga, N C.; Sugie, A.; Nomiya, K. *J. Chem. Soc., Dalton Trans.* **2004**, *21*, 3732−3740.

(23) (a) Podsiadlo, P.; Paternel, S.; Rouillard, J. M.; Zhang, Z.; Lee, J.; Lee, J. W.; Gulari, E.; Kotov, N. A. *Langmuir* **2005**, *21*, 11915−11921. (b) Lu, Y.; Liu, G. L.; Lee, L. P. *Nano Lett.* **2005**, *5*, 5−9.

(24) Heilmann, A. *Polymer Films with Embedded Metal Nanoparticles*; Springer-Verlag: New York, 2002.

(25) (a) Dowling, D. P.; Betts, A. J.; Pope, C.; McConnell, M. L.; Eloy, R.; Arnaud, M. N. *Surf. Coat. Technol.* **2003**, *163*, 637−640. (b) Affinito, J.; Martin, P.; Gross, M.; Coronado, C.; Greenwell, E. *Thin Solid Films* **1995**, *270*, 43−48. (c) Dowling, D. P.; Donnelly, K.; McConnell, M. L.; Eloy, R.; Arnaud, M. N. *Thin Solid Films* **2001**, *398−399*, 602−606.

(26) (a) Jiang, H.; Manolache, S.; Wong, A. C. L.; Denes, F. S. *J. Appl. Polym. Sci.* **2004**, *93*, 1411−1422. (b) Favia, P.; Vulpio, M.; Marino, R.; D'Agostino, R.; Mota, R. P.; Catalano, M. *Plasmas Polym.* **2000**, *5*, 1−14.

(27) Lide, D. R. *CRC Handbook of Chemistry and Physics*, 83rd ed.; CRC Press: Boca Raton, FL, 2002.

(28) (a) Tiller, J. C.; Liao, C. J.; Lewis, K.; Klibanov, A. M. *Proc. Natl. Acad. Sci. U.S.A.* **2001**, *98*, 5981−5985. (b) Tiller, J. C.; Lee, S. B.; Lewis, K.; Klibanov, A. M. *Biotechnol. Bioeng.* **2002**, *79*, 465−471.

(29) Li, G.; Shen, J.; Zhu, Y. *J. Appl. Polym. Sci.* **1998**, *67*, 1761−1768.

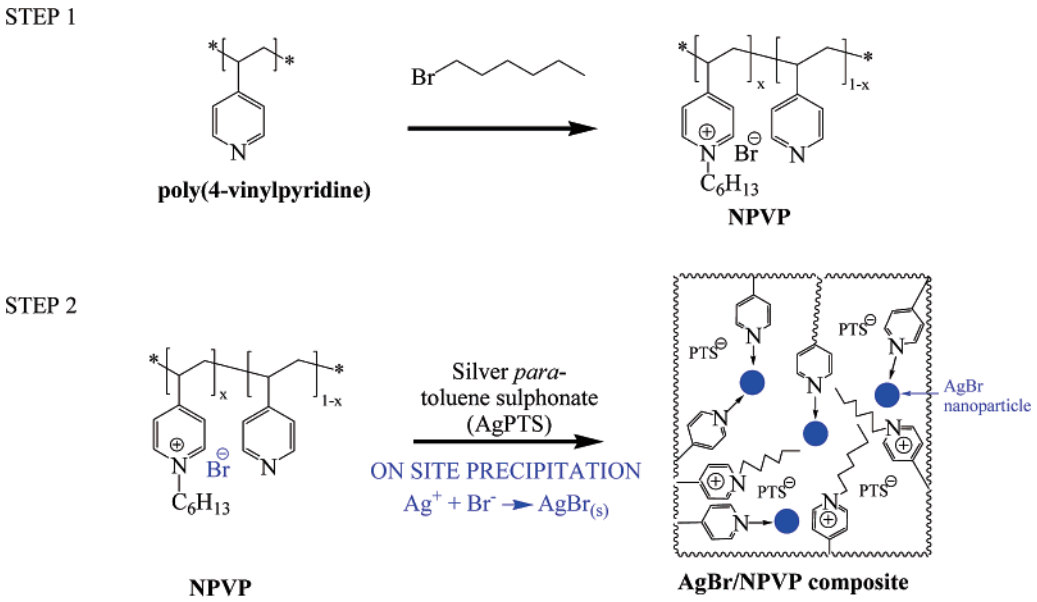

Figure 1. Schematic of on-site precipitation method for the synthesis of dual action antibacterial composite material, AgBr/**NPVP** (**NPVP** = poly(4-vinylpyridine)-*co*-poly(4-vinyl-*N*-hexylpyridinium bromide).

used in synthesis of nanoparticles,[30] to the best of our knowledge this is the first example of use of precipitation technique to directly synthesize polymer/nanoparticle composites in a single step. The starting polymer, poly(4-vinylpyridine)-*co*-poly(4-vinyl-*N*-hexylpyridinium bromide), **NPVP**, was prepared by partially N-alkylating the pyridine nitrogens of commercially available polymer poly(4-vinylpyridine) (MW: 60 000) using a slight modification of a process described elsewhere.[28a] Two different starting **NPVP** polymers with 21 and 43% N-alkylation were synthesized and characterized by ^{1}H NMR spectroscopy. Then the bromide counteranion of **NPVP** was precipitated on-site as silver bromide by the slow addition of silver *para*-toluenesulfonate solution to the polymer solution, yielding composites abbreviated as AgBr/21% **NPVP** and AgBr/43% **NPVP**, respectively. For each **NPVP** polymer, two different AgBr/**NPVP** composites with silver ion to polymer bromide ion molar ratios of 1:2 and 1:1 were prepared by adding different amounts of silver *para*-toluenesulfonate. The 1:2 composites yielded clear yellow solutions, whereas the 1:1 composites gave translucent yellow colloidal solutions. Both solutions were stable at room temperature for up to 5 d. Solid AgBr/**NPVP** composites were obtained by precipitation upon addition to diethyl ether. Thus, four different AgBr containing composites, 1:1 AgBr/21% **NPVP**, 1:2 AgBr/21% **NPVP**, 1:1 AgBr/43% **NPVP**, and 1:2 AgBr/43% **NPVP**, were prepared and studied. Solid AgBr/**NPVP** composites could be redissolved in methanol, ethanol, nitromethane, or DMSO to give back the clear/colloidal solutions. The composite solutions in methanol were used to form coatings on glass.

The adhesive properties of AgBr/**NPVP** composite films on glass were evaluated using the standard Scotch tape test.[31] Standard-sized microscope glass slides were cleaned with 3:1 sulfuric acid/30% hydrogen peroxide and were coated with 5 wt % solution of the composites in methanol using a Laurell WS 400B spin coater at 1500 rpm. A strip of Scotch tape (3M-Catalog No. 810) was placed over the coated surface and was rubbed in with continuous motion to attach it firmly to the slide. The strip was then peeled off by lifting the tape from one end to the other. The slide and the tape were then visually inspected under a dissecting microscope (Olympus S7-PT) to observe any peeling from the surface of glass or any pieces sticking to the tape. Almost negligible peeling was observed in all of the AgBr/**NPVP** composite films. Glass surfaces are negatively charged due to the presence of surface Si−O$^-$ groups. Hence, strong adhesion is expected due to electrostatic attraction between the glass and the cationic polymer.

Solid composite monoliths were sectioned into thin slices to enable electron microscopy imaging. TEM images clearly indicate the presence of spherical nanoparticles embedded inside the solid polymer and suggest that precipitation is taking place on-site very close to the polymer chains (Figure 2). If AgBr had precipitated in solution away from the polymer chains, high and uniform distribution of nanoparticles throughout the polymer matrix would not have been expected. Since the precipitation takes place in the vicinity of the polymer chains, the growing AgBr nanoparticles are stabilized and prevented from aggregating by the capping action of the coordinating pyridine groups. Steric isolation by the comb-shaped polymer also helps in the stabilization of the nanoparticles. Similar stabilization of nanoparticles in polymer matrixes has been documented previously for metal nanoparticles in polysiloxane solutions.[32] Both the degree of polymer N-alkylation (21 versus 43%) and bromide to added silver molar ratio (1:1 versus 1:2) had significant effect on the size of embedded nanoparticles (Table 1, Figure 2). The lower the degree of N-alkylation of the polymer (21 versus 43%), the smaller the resulting nanoparticles. This can be attributed to a higher proportion of coordinating pyridine groups in 21% **NPVP** over 43% **NPVP**, which would result in higher capping efficiency for the growing nanoparticles. For the **NPVP** polymer, the lower the Ag^+ to Br^- (polymer) ratio (1:2 versus

(30) (a) Cushing, B. L.; Kolesnichenko, V. L.; O'Connor, C. J. *Chem. Rev.* **2004**, *104*, 3893−3946. (b) Burda, C.; Chen, X.; Narayanan, R.; El-Sayed, M. L. *Chem. Rev.* **2005**, *105*, 1025−1102.
(31) Guiseppi-Elie, A.; Brockmann, T. W. *Langmuir* **1995**, *11*, 1768−1776.
(32) (a) Chauhan, B. P. S.; Rathore J. S. *J. Am. Chem. Soc.* **2005**, *127*, 5790−5791. (b) Chauhan, B. P. S.; Rathore, J. S.; Bandoo, T. *J. Am. Chem. Soc.* **2004**, *126*, 8493−8500. (c) Rathore, J. S.; Abdelwahed, S. H.; Guzei, I. A. *J. Am. Chem. Soc.* **2003**, *125*, 8712−8713.

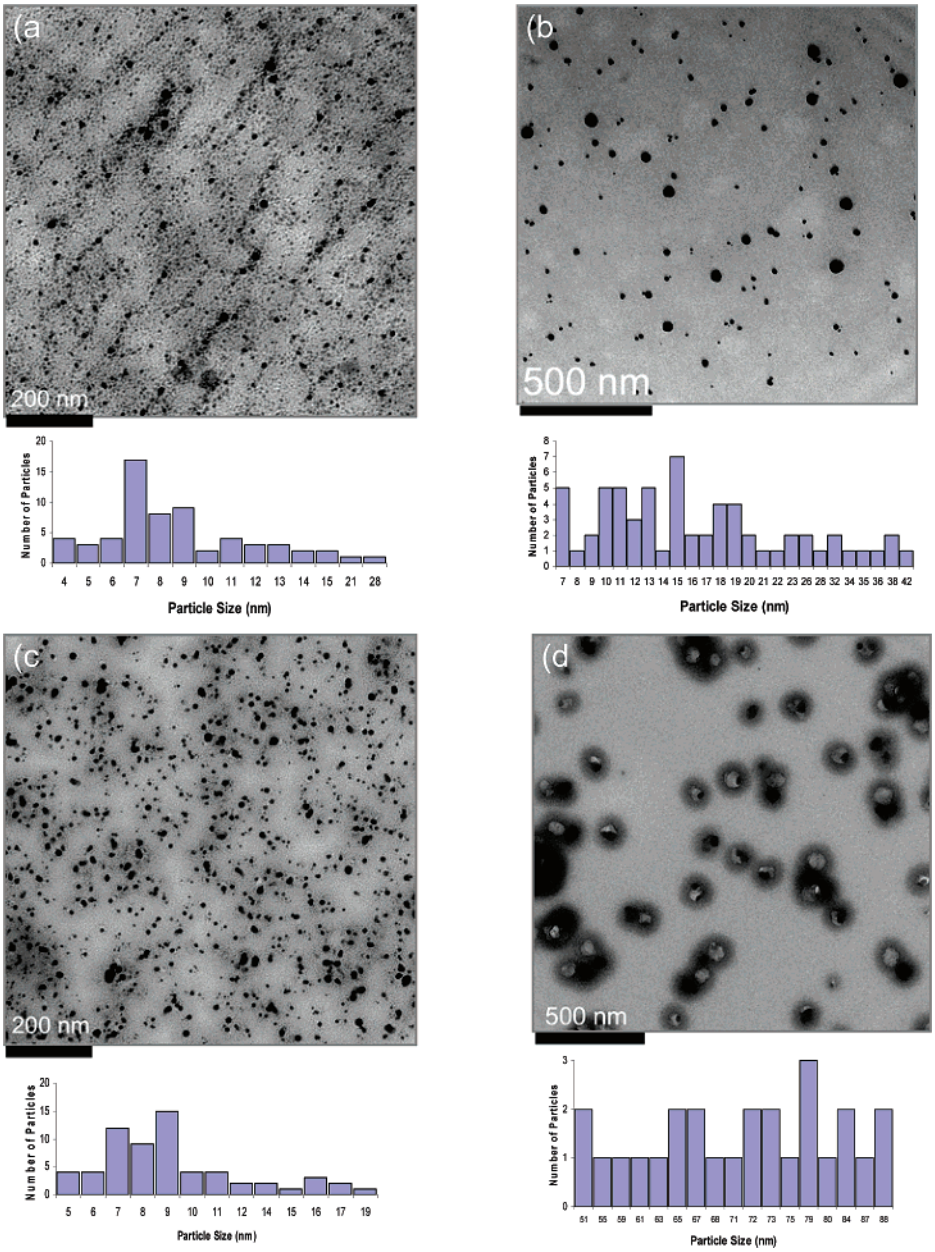

Figure 2. TEM images with particle-size histograms of microsections of the solid AgBr/**NPVP** composites. (a) 1:2 AgBr/21% **NPVP**, (b) 1:1 AgBr/21% **NPVP**, (c) 1:2 AgBr/43% **NPVP**, and (d) 1:1 AgBr/43% **NPVP**.

Table 1. Average Particle Sizes for AgBr/21% **NPVP** and AgBr/43% **NPVP** Composites[a]

	% N-alkylation	
Ag/Br ratio in composite	43% average AgBr size (nm)	21% average AgBr size (nm)
1:2	10 (4)	9 (4)
1:1	71 (11)	17 (9)

[a] Standard deviations are given in parentheses.

1:1) the smaller the nanoparticles. This is presumably a result of lower AgBr/capping agent ratio in the former. Interestingly, there appears to be a lower size limit for the AgBr particles since the 1:2 composites of both 21% **NPVP** and 43% **NPVP** have similar sized particles.

Energy-dispersive X-ray spectroscopy (EDS) and powder X-ray diffraction (XRD) were employed to establish the chemical identity of the observed nanoparticles. EDS spectra of the composite sections were taken during TEM imaging. The electron beam was focused on an approximately 100 nm × 100 nm particle-rich region, and backscattered X-ray information was collected to get qualitative elemental information about the composite sections. The EDS spectra showed the presence of significant amounts of silver and bromine (Figure 3), consistent with the presence of AgBr nanoparticles. The sulfur signal is from the *para*-toluenesulfonate counterion. The Cu, Fe, and Cr signals are from the TEM grid.

To establish whether the nanoparticles were those of AgBr or some other silver species such as oxide or metallic silver, XRD spectra of 1:1 AgBr/43% **NPVP** and 1:1 AgBr/21% **NPVP** were recorded. The XRD diffraction patterns (Figure 4) are consistent with the presence of cubic AgBr (Bromargyrite, $Z = 4$, space group *Fm*-3*m*).[33]

To quantify the amount (wt %) of AgBr present in the composites, thermogravimetric analyses of the 1:1 and 1:2

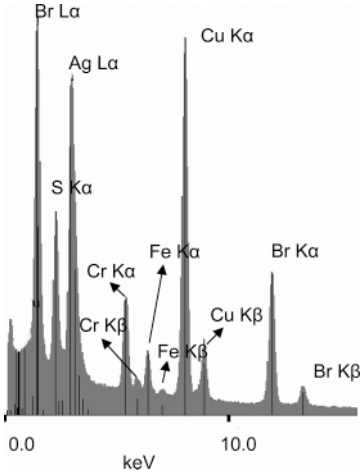

Figure 3. EDS of 1:1 AgBr/43% **NPVP** microsection showing the presence of significant amounts of Ag and Br.

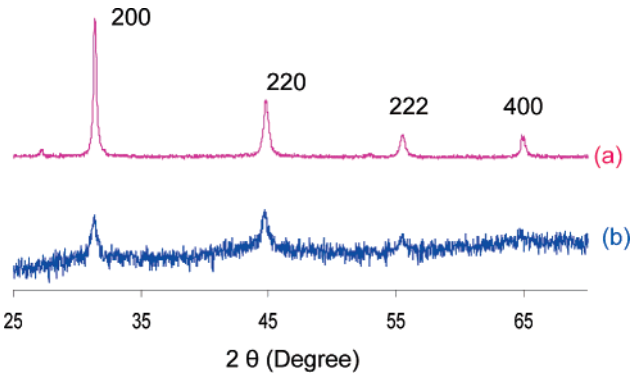

Figure 4. X-ray diffraction pattern of (a) 1:1 AgBr/43% **NPVP** composite having an average AgBr particle size of 71 nm and (b) 1:1 AgBr/21% **NPVP** composite having an average AgBr particle size of 17 nm.

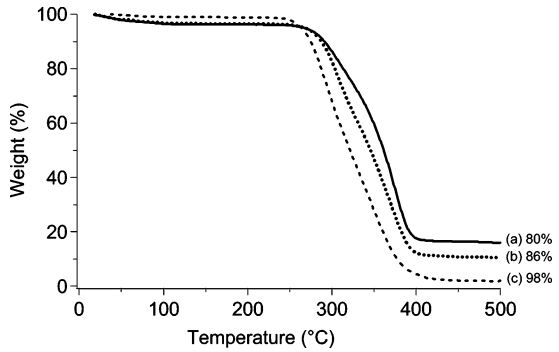

Figure 5. Thermogravimetric analysis curves showing % wt loss between 200 and 450 °C. (a) 1:1 AgBr/21% **NPVP**, (b) 1:2 AgBr/21% **NPVP**, and (c) pure 21% **NPVP**.

AgBr/21% **NPVP** composites were performed using a heating rate of 20 °C/min under an argon flow of 100 mL/min. The sharp weight loss between 250 and 400 °C corresponds to the decomposition of the polymer matrix, leaving AgBr residue (Figure 5). The pure 21% **NPVP** polymer left negligible residue as char (2%). After accounting for 2% of residual char due to the polymeric **NPVP** matrix, we estimated the weight percent of AgBr in the 1:1 composite to be 18% (80% weight loss between 200 and 450 °C) and 12% (86% weight loss between 200 and 450 °C) for the 1:2 composite. This was in good agreement with theoretically calculated values of residual AgBr in the 1:1 and 1:2 composites (19.9 and 11.7 wt %, respectively). Thus, the precipitated AgBr is quantitatively embedded inside the polymer matrix during the synthetic step and is not lost as some soluble species. The presence of silver was also quantified further using elemental analysis by atomic absorption spectroscopy of digested composite samples in aqua regia (Perkin-Elmer 703). The Ag contents in 1:1 and 1:2 AgBr/21% **NPVP** were found to be 10.1 and 6.3 wt %, respectively, which agreed with the theoretical values of 11.4 and 6.7 wt %, respectively.

2.2. Antibacterial Effect. All antibacterial activity tests were performed in triplicate and were done at least two different times to ensure reproducibility. The antibacterial properties of the composites were tested against gram-positive *Bacillus cereus* and *Staphylococcus aureus* and gram-negative *Escherichia coli* and *Pseudomonas aeruginosa*.

2.2.1. Surface and Airborne Bacteria. A modified Kirby Bauer disk diffusion technique as described previously by Melaiye et al.[22a] was used to probe the bactericidal effect of the composites. Identically sized filter papers were coated with the same amount of AgBr/43% **NPVP** composite solutions in methanol and were dried. These filter papers were then placed on bacteria-inoculated agar plates and were visualized for antibacterial activity after being incubated overnight. The bacteria spread on agar plates closely resemble real world situations in which pathogenic bacteria are often present on receptive nutrient surfaces in biomedical implants, medical devices, or food packaging surfaces. The **NPVP**/AgBr composites placed on the bacteria-inoculated surfaces killed all the bacteria under and around them. We observed distinct zones of inhibition (clear areas with no bacterial growth) around the composite samples for both *E. coli* and *B. cereus* (Figure 6a−d). High bacterial growth as indicated by bacterial growth lawn (large indistinguishable collection of colonies) was observed everywhere else. Also, no bacterial growth was observed under or within the composites. Controls consisting of sodium *para*-toluenesulfonate and 21 and 43% **NPVP** impregnated filter papers exhibited no zones of inhibition. The poor solubility of 43% **NPVP** in LB broth, coupled with slow diffusion of the comb-shaped polymer macromolecule through solid agar, results in the lack of a zone of inhibition. On the other hand, Ag^+ ions are highly soluble in LB broth and can diffuse readily, thereby exhibiting a clear zone of inhibition. However, 43% **NPVP** does kill bacteria in the presence of liquid LB broth, although much less effectively than AgBr/**NPVP** composites (Table 3).

We also tested the ability of these composites to serve as antibacterial coatings on surfaces. The antibacterial activity of coated glass slides toward airborne *E. coli* was tested using a slight modification of assay described by Tiller et al.[28a] Glass slides were partially coated by evaporating 3 × 50 μL of 5 wt % composite solution in methanol. Airborne *E. coli* bacteria were then sprayed on the surface of the coated disks, and bacterial growth was visualized after overnight incubation in LB agar. No bacterial growth was observed on top of the coatings or adjacent to the coatings (zone of inhibition) (Figure 6e). Bacterial growth was seen on uncoated glass surface as indicated by the presence of colonies. In both the Kirby Bauer testing with composite-coated paper and glass slide testing, the observed zone of inhibition is a result of the leaching of active

(33) Takahashi, H.; Tamaki, S.; Sato, S. *J. Phys. Soc. Jpn.* **1987**, *56*, 3593−3597.

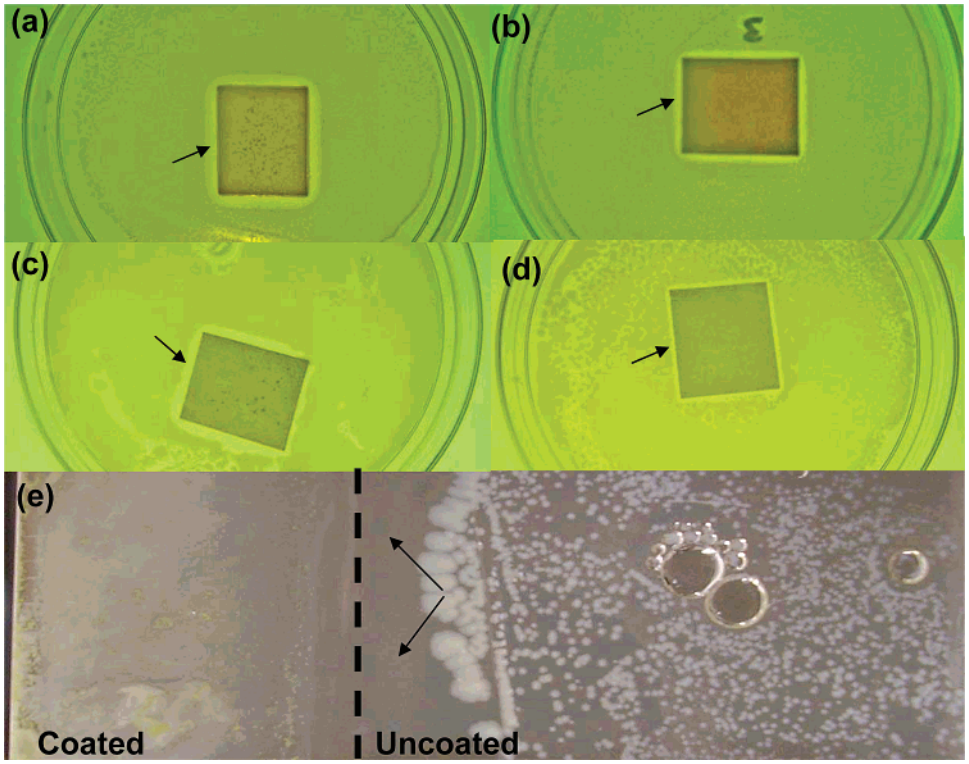

Figure 6. Antibacterial activity of AgBr/**NPVP** composites. Zone of inhibition is indicated by arrows. (a) 1:2 AgBr/43% **NPVP** composite-coated paper placed on the LB agar plate inoculated with *E. coli* showing a comparatively large zone of inhibition, (b) 1:1 AgBr/43% **NPVP** composite showing a comparatively small zone of inhibition, (c) 1:2 AgBr/43% **NPVP** composite-coated paper placed on the LB agar plate inoculated with *B. cereus* showing a comparatively large zone of inhibition, and (d) 1:1 AgBr/43% **NPVP** composite showing a comparatively small zone of inhibition. (e) Glass slide coated with 1:1 AgBr/21% **NPVP** and sprayed with airborne *E. coli* mist also exhibiting a zone of inhibition. *E. coli* colonies can be seen in uncoated area.

Table 2. Correlation of the Size of the Zone of Inhibition with the AgBr Particle Size in AgBr/43% **NPVP** Composites[a]

AgBr particle size (nm)	zone of inhibition *E. coli* (mm)	zone of inhibition *B. cereus* (mm)
10 (4)	3.1 (0.1)	2.3 (0.7)
71 (11)	1.9 (0.2)	0.9 (0.1)

[a] Standard deviations are given in parentheses.

biocidal species Ag^+ ion from the embedded AgBr nanoparticles present in the composite into the surrounding aqueous medium. The presence of the inhibition zone clearly indicates that the mechanism of the biocidal action of the composite is not merely due to membrane disruption by the ampiphilic **NPVP** but also due to the leached Ag^+ ion.

The sizes of the zones of inhibition for different AgBr/43% **NPVP** composites are given in Table 2. Interestingly, the size increased with decreasing size of the AgBr nanoparticles. We attribute this to higher rate of leaching from the smaller particles due to their higher surface-to-volume ratio. Thus, it is possible to control the leaching rate of Ag^+ ion by varying the size of the embedded AgBr particles.

Atomic emission spectrometry further indicated that for the same weight of AgBr, composites with smaller AgBr nanoparticles produced a higher concentration of Ag^+ ions in the surrounding medium than composites with larger AgBr nanoparticles. 1:1 and 1:2 AgBr/43% **NPVP** composites were selected for this study due to the size difference in the AgBr nanoparticle present in them (71 and 10 nm, respectively). TGA analysis of composites indicated the presence of 18.9 wt % AgBr in the 1:2 composite and 28.3 wt % AgBr in the 1:1 composite. Measured weights of 1:1 and 1:2 AgBr/43% **NPVP** composites were incubated with calculated volumes of LB broth, such that the ratio between the volume of LB broth (mL) and weight of AgBr (g) was kept constant. The concentration of soluble Ag^+ in broth was then measured by emission spectrometry. The 1:2 composites generated a higher average soluble Ag^+ concentration of 3.65 ± 0.47 ppm/g AgBr, whereas the 1:1 composite generated a smaller soluble Ag^+ concentration of 2.84 ± 0.44 ppm/g AgBr. Thus, concentrations of soluble species generated from the 1:2 composite (AgBr size, 10 nm) were higher than concentrations from the 1:1 composite (AgBr size, 71 nm).

2.2.2. Waterborne Bacteria. The relative antibacterial activities of AgBr/**NPVP** composites, **NPVP** alone, and AgBr alone toward gram-negative *E. coli* and gram-positive *B. cereus* were studied in aqueous LB broth using the minimum inhibitory concentration (MIC) test. A standard testing protocol for water-insoluble antimicrobials was used.[33] MIC is the lowest concentration (μg/mL) at which a compound will kill more than 99% of the added bacteria. A lower MIC corresponds to a higher antibacterial effectiveness. Different weights of AgBr/**NPVP** composites, **NPVP** alone, and AgBr alone, corresponding to anticipated MIC values of 50−10 000 μg/mL, were incubated with *E. coli* and *B. cereus* in aqueous LB broth. Bacterial growth was studied by visually inspecting the LB broth for turbidity (bacterial growth causes clear LB broth to turn turbid). Lack of turbidity may correspond to either very low bacterial growth (bacteriostatic effect) or complete killing of bacteria (bactericidal effect). To establish whether the composites were bacteriostatic or bactericidal, 100-μL aliquots were taken from the incubated LB broth and were plated on nutrient agar plates. The plates

Table 3. Comparison of the Antibacterial Activity (Minimum Inhibitory Concentration, MIC) of AgBr/**NPVP** Composites, **NPVP**, and AgBr alone toward Gram-Negative *E. coli* and Gram-Positive *B. cereus*

	MIC (μg/mL)		LB broth turbidity after 18 h of incubation[a]		colonies on agar plate after plating 100 μL of aliquot	
sample	*E. coli*	*B. cereus*	E. coli	B. cereus	E. coli	B. cereus
1:2 AgBr/21% **NPVP**	50	50	clear	clear	none[b]	none[b]
1:1 AgBr/21% **NPVP**	50	50	clear	clear	none	none
1:2 AgBr/43% **NPVP**	50	50	clear	clear	none	none
1:1 AgBr/43% **NPVP**	50	50	clear	clear	none	none
21% **NPVP**	1000	1000	clear	turbid	45[c]	lawn[d]
43% **NPVP**	250	250	clear	clear	11[c]	none
AgBr	100	100	clear	clear	none	none
Na PTS[e]	10000	10000	turbid	turbid	lawn	lawn
PVP[e]	10000	10000	turbid	turbid	lawn	lawn

[a] LB broth before incubation was clear with bacterial concentration of 5×10^5 cfu/mL; after 18 h incubation clear = no bacterial growth, turbid = large bacterial growth. [b] No colonies imply the material is bactericidal. [c] Visible colonies imply the species is bacteriostatic at the given concentration. [d] Lawn denotes a large indistinguishable collection of colonies indicating high bacterial growth in the plated aliquot. [e] NaPTS: Sodium *para*-toluenesulfonate; PVP: poly(4-vinylpyridine).

Table 4. Comparison of Extended Antibacterial Activity of AgBr/21% **NPVP** Composites with that of AgBr and 21% **NPVP** alone

	concn of sample in	concn of AgBr[b]	*E. coli* growth[a]			*B. cereus* growth[a]		
sample	4 mL of LB broth (μg/ mL)	(μg/mL)	day 1	day 3	day 17	day 1	day 3	day 17
1:1 AgBr/21% **NPVP**	500	90	−	−	−	−	−	−
1:2 AgBr/21% **NPVP**	500	60	−	−	−	−	−	−
AgBr	250	250	−	+(107)	+++	−	+(154)	+++
21% **NPVP**	1000	0	+(169)	+++	+++	+(209)	+++	+++

[a] Cell growth was quantified by visual inspection (LB broth turbidity) and by counting colonies after plating 100 μL of broth. − = no growth indicating bactericidal effect. + = LB broth clear; bacteriostatic effect with the number of colonies observed on plating of aliquot given in parentheses. ++ = LB broth clear; number of colonies observed on plating of aliquot too large to count. +++ = LB broth turbid; lawn of colonies observed on plating of aliquot. [b] 1:1 and 1:2 AgBr/21% **NPVP** composites have 18 and 12 wt % of AgBr, respectively, as shown by TGA.

were then incubated at 37 °C (*E. coli*) or 30 °C (*B. cereus*) for 16−20 h, and colonies were counted. Bacterial colonies indicate the presence of live bacteria in the aliquots that were plated. If the material being tested does not kill but inhibits the growth of bacteria (bacteriostatic), bacteria will grow when removed from the solution containing the material and the colonies will be observed upon plating the aliquot. If the material being tested is bactericidal, no bacterial colonies would be observed upon plating. The results are given in Table 3. All the AgBr/**NPVP** composites were bactericidal at MIC of 50 μg/mL. AgBr alone was bactericidal at MIC of 100 μg/mL. The 21 and 43% **NPVP** were antibacterial at the much higher MIC values of 1000 and 250 μg/mL, respectively. Poly(4-vinylpyridine) and sodium *para*-toluenesulfonate were ineffective even at 10 000 μg/mL and showed large bacterial growth. Clearly, the AgBr/**NPVP** composites exhibit a higher antibacterial activity than 21 or 43% **NPVP** polymer alone for both *E. coli* and *B. cereus*. These tests also support the dual action mechanism of antibacterial activity viz. the bactericidal effect of Ag^+ and membrane-disrupting effect of the ampiphilic cationic polymer.

2.2.3. Long-Lasting Antibacterial Action. The antibacterial properties of the materials in aqueous LB medium were tested over an extended period of time. Solid 1:1 and 1:2 AgBr/21% **NPVP** composites, 21% **NPVP** alone, and AgBr alone in LB broth were inoculated daily with freshly grown bacteria. At the end of each inoculation/incubation cycle (18−20 h), the LB broth was inspected for bacterial growth (turbidity). A quantity of 100 μL of the medium was then plated on LB agar plates and incubated to visualize bacterial colonies. This was done to differentiate between bactericidal and bacteriostatic effect in cases where LB broth was still clear. At the end of each daily cycle, the old LB broth was discarded and fresh LB-bacteria suspension was added. This protocol allowed us to unambiguously test the ability of the composites to generate sufficient amounts of bioavailable Ag^+ ion each day without getting depleted. Bioavailable silver released each day would be removed with the old LB, and the ability of the composite to generate more active species would be tested. Simply adding fresh bacteria without removing the old LB solution would not prove the ability of the composites to generate active silver species as silver was not being removed from the medium. As can be seen in Table 4, both the 1:2 and 1:1 AgBr/21% **NPVP** composites were completely bactericidal (no colony formation on plating) until 17 d. AgBr was bactericidal for the first two inoculations, bacteriostatic from day 3 to day 15 (i.e., LB broth remained clear but colonies were observed on plating), and ineffective from day 15. Thus, clearly both the 1:1 and 1:2 AgBr/21% **NPVP** composites sustained a sufficient concentration of bioavailable Ag^+ ions in the medium for days to kill both *E. coli* and *B. cereus*. It is interesting to note that, even though the tested AgBr/21% **NPVP** composites had a lower amount of AgBr per milliliter of bacterial cell suspension (90 and 60 μg/mL encapsulated AgBr in the composites versus 250 μg/mL for AgBr alone), the composites were bactericidal for a longer amount of time than AgBr alone. The 21% **NPVP** alone was bacteriostatic on day 1 and was ineffective after that. The reason for this short duration of 21% **NPVP** can be explained as follows. The mechanism for antibacterial action of cationic **NPVP** polymers is bacterial membrane disruption by the polymers.[4g] Also, **NPVP** polymers have been shown to have bacteria-adsorbing effects (capture of negatively charged bacteria by cationic polymer).[4a] Once the polymer kills/captures the bacteria, the cell membrane remnants/dead bacteria presumably remain tightly adsorbed on the polymer surface preventing further antibacterial action. In contrast, AgBr/**NPVP** composites continue to release Ag^+ ions into the medium even after the

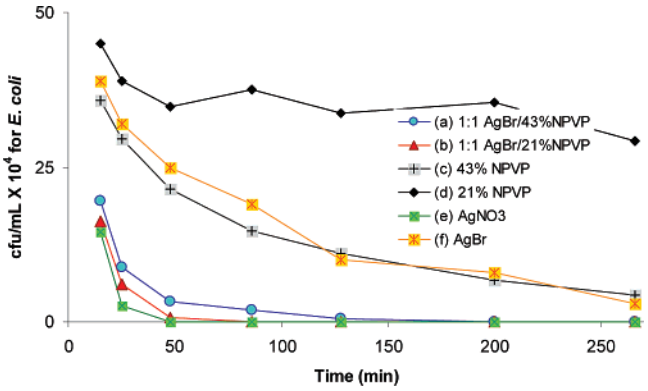

Figure 7. Kinetics of antibacterial activity of different silver species and polymers toward *E. coli*. Concentration of each species in LB broth bacterial suspension was as follows: (a) 100 μg/mL (contains 18 μg/mL of AgBr), (b) 100 μg/mL (contains 12 μg/mL of AgBr), (c) 250 μg/mL, (d) 1000 μg/mL, (e) 18 μg/mL, molar equivalent of silver present in 1:1 AgBr/43% **NPVP**, (f) 100 μg/mL.

surface is completely covered by dead bacteria, thereby showing long-lasting activity.

2.2.4. Antibacterial Kinetics. Finally, the kinetics of antibacterial activity of different composites and polymers toward *E. coli* were investigated. The AgBr-containing composites are antibacterial because of the leaching of the Ag^+ ion and the membrane-disrupting property of the ampiphilic cationic polymer. The antibacterial kill rates of 1:1 AgBr/43% **NPVP** and 1:1 AgBr/21% **NPVP** composites were compared with those of ionic silver species and cationic polymers alone. Known amounts of each species (i.e., 1:1 AgBr/43% **NPVP**, 1:1 AgBr/21% **NPVP**, 43% **NPVP**, 21% **NPVP**, $AgNO_3$, and AgBr) were separately incubated with 4 mL of *E. coli* in LB broth in 15-mL culture tubes (*E. coli* concentration, 5×10^5 cfu/mL) to yield a series of suspensions. Aliquots from each suspension were withdrawn at set time intervals, plated on LB agar plates and incubated overnight. Colonies formed after overnight incubation were counted, and these corresponded to the number of live bacteria in each suspension at the time of aliquot withdrawal. A plot of colony-forming units (cfu/mL) of *E. coli* versus time was constructed (Figure 7) to visualize the kill rates of each species. As Figure 7 shows, the composites had a much faster bacterial suppression rate at a lower equivalent concentration (faster reduction in number of colony-forming units with time) than both the polymers and AgBr alone. The 1:1 AgBr/21% **NPVP** composite has a slightly faster suppression rate than the 1:1 AgBr/43% **NPVP** composite. This is again due to the smaller AgBr particles in the 1:1 AgBr/21% composite leaching at a faster rate. Interestingly, the kinetics for both the composites were nearly as fast as that for water-soluble $AgNO_3$. The advantage of the composites lies in their extended time-release properties. Thus, by encapsulating AgBr nanoparticles in the cationic ampiphilic polymer matrix, one can achieve both fast and long-lived antibacterial effectiveness.

2.2.5. Performance in Mammalian Systems. A major concern of the health industry is surface-centered infections associated with implants and biomedical devices coming in contact with body fluids. Hence, we decided to briefly investigate the antibacterial activity of AgBr/**NPVP** composites toward methicillin-resistant *S. aureus* after exposure to mammalian fluids. *S. aureus* is a clinically relevant gram-positive bacterium that is difficult to kill and has been implicated in a range of infections related to biomedical device and implant use in human patients.[34] Different weights of AgBr/**NPVP** composites and **NPVP** alone corresponding to anticipated MIC values of 50−10 000 μg/mL were incubated with three different mammalian fluids (human serum, human saliva, and human blood) for 5 h at room temperature. A suspension of methicillin-resistant *S. aureus* (5×10^5 cfu/mL) in minimum essential medium (MEM) containing 30% v/v human serum was then added to the composites. The contents were incubated for 18−20 h to allow bacterial growth. To quantify the bacteriostatic or bactericidal effect, 100-μL aliquots were plated on nutrient agar plates and incubated at 37 °C for 16−20 h. Plates were then visually inspected for any colony formation. Bacterial colonies indicate the presence of viable bacteria in the aliquots that were plated. The results are given in Table 5. All the composites retained antibacterial activity after exposure to mammalian fluids. Also, the composites did not lose their antibacterial activity in the presence of growth medium containing 30% human serum. Polymer controls 21 and 43% **NPVP** were completely ineffective in killing bacteria after exposure to human serum and blood. Presumably negatively charged proteins and macromolecules in human serum and blood tightly bind to the cationic polymers, thereby deactivating them toward membrane disruption of bacteria. However, in the case of AgBr/**NPVP** composites, Ag^+ ions are still generated and the composites exhibit potent antibacterial effect. However, the composites are more active in the absence of mammalian fluids; composites exhibited a MIC of 50 μg/mL toward methicillin-resistant *S. aureus* in LB broth. This decrease in activity in the presence of mammalian fluids may be attributed to the partial capture of soluble biocidal Ag^+ ions by coordinating groups (thiols, acids, etc.) of proteins and other macromolecules present in mammalian fluids.

2.2.6. Biofilm Formation. The ability of AgBr/**NPVP** composite-coated surfaces to resist biofilm formation was evaluated using scanning electron microscopy (SEM), a well-known technique to study biofilm formation.[35] *P. aeruginosa* is gram-negative bacteria that is widely present in the environment and is known to form tough biofilms on most surfaces.[36] *P. aeruginosa* biofilms have been implicated in chronic lung infections in patients suffering from cystic fibrosis.[37] Glass surfaces were coated with 1:1 AgBr/21% **NPVP** and 21% **NPVP** alone. These were then incubated for 24−72 h with *P. aeruginosa* suspension (1×10^7 cfu/mL) in LB broth. Fresh bacterial suspension was added after every 24 h. The coated slides were removed from the bacterial suspension after 24, 48, and 72 h, and SEM images of surfaces were recorded after fixation to study the extent of biofilm formation. Extensive biofilm formation was observed on 21% **NPVP**-coated surfaces (Figure 8a,b). Nearly the entire surface was covered with compact bacterial biofilm after 48 h of incubation. No biofilm

(34) (a) Hudson, M. C.; Ramp, W. K.; Frankenburg, K. P. *FEMS Microbiol. Lett.* **1999**, *173*, 279−284. (b) Harris, L. G.; Richards, R. G. *J. Mater. Sci.*: *Mater. Med.* **2004**, *15*, 311−314.
(35) (a) Ramage, G.; Walle, K. V.; Wickes, B. L.; Lopez-Ribot, J. L. *J. Clin. Mirobiol.* **2001**, *39*, 3234−3239. (b) Andes, D.; Nett, J.; Oschel, P.; Albrecht, R.; Marchillo, K.; Pitula, A. *Infect. Immun.* **2004**, *72*, 6023−6031.
(36) Tolker-Nielsen, T.; Molin, S. *Pseudomonas*; Kluwer Academic/Plenum Publishers: New York, 2004; pp 547−571.
(37) (a) Moskowitz, S. M.; Foster, J. M.; Emerson, J. C.; Gibson, R. L.; Burns, J. L. *J. Antimicrob. Chemother.* **2005**, *56*, 879−886. (b) Landry, R. M.; An, D.; Hupp, J. T.; Singh, P. K.; Parsek, M. R. *Mol. Microbiol.* **2006**, *59*, 142−151.

Table 5. Antibacterial Activity of AgBr/**NPVP** Composites toward *S. aureus* after Exposure to Mammalian Fluids

sample	human serum	human saliva	human blood
AgBr/21% **NPVP** and AgBr/43% **NPVP** composites	bactericidal[a] at 150 μg/mL; bacteriostatic[b] at 100 μg/mL	bactericidal[a] at 100 μg/mL; bacteriostatic[b] at 50 μg/mL	bactericidal[a] at 200 μg/mL; bacteriostatic[b] at 100 μg/mL
43% **NPVP**	lawn[c]	bactericidal[a] at 1000 μg/mL	lawn[c]
21% **NPVP**	lawn[c]	bactericidal[a] at 5000 μg/mL	lawn[c]

[a] Bactericidal: <10 colonies observed after plating 100 μL; sample kills >99.99% bacteria at the given concentration. [b] Bacteriostatic: ~300−400 colonies observed on plating 100 μL; sample kills/inhibits growth of >98% bacteria. [c] Lawn denotes a large indistinguishable collection of colonies on agar plate indicating high bacterial growth in the plated aliquot; the sample is not active at 10,000 μg/mL,

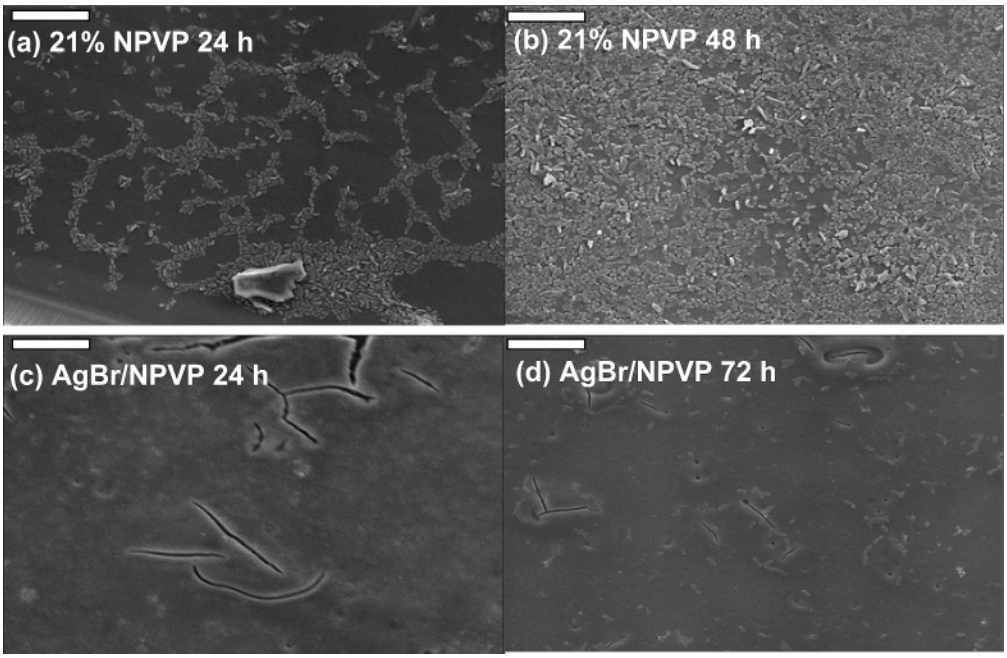

Figure 8. SEM image of coated glass surfaces after incubation with *P. aeruginosa*. (a), (b) Biofilm on 21% **NPVP**-coated glass surfaces after 24 and 48 h incubation. Dense collection of rod-shaped bacteria can be seen colonizing the surface. (c), (d) No biofilm formation observed on 1:1 AgBr/21% **NPVP**-coated glass surfaces even after 72 h incubation. Scale bar is 10 μm.

formation was observed on 1:1 AgBr/21% **NPVP**-coated surfaces after 72 h (Figure 8c,d). Although a few bacteria were found scattered all over the surface, no colonization or bacterial aggregation was observed for the silver-containing composite. The cationic polymer 21% **NPVP** will initially kill bacteria in immediate contact with its surface due to its membrane-disrupting effect. However, dead cells and cellular debris adhering to the positively charged polymer surface would attenuate any further membrane-disrupting action. Moreover, dead cells and debris on the surface of the polymer provide an organic conditioning layer, a necessary first step in biofilm formation.[38] Hence, a compact biofilm forms on 21% **NPVP**-coated surfaces. In the case of AgBr/**NPVP**-coated surfaces, constant diffusion of the Ag^+ ion creates an antibacterial zone extending some distance beyond the immediate surface and hence prevents biofilm formation.

3. Conclusions

In summary, we have described a novel dual action antibacterial material composed of a cationic polymer and silver bromide nanoparticles. A relatively easy synthesis was used to fabricate the material. The composites were capable of killing both gram-negative and gram-positive bacteria on surfaces and in solution. The kill rates of these composites were comparable to that of highly active soluble silver salts. Additionally, the composites gave a sustained release of biocidal silver ion in aqueous LB media and were bactericidal for days without loss of activity. The rate of release of the biocidal Ag^+ ion can be tuned by varying the size of the polymer-embedded nanoparticles. The AgBr/**NPVP** composites retained their antibacterial activity after exposure to mammalian fluids and also inhibited biofilm formation. These composites may find use as antimicrobial coatings for a wide variety of biomedical and general use applications. Further variations in the antibacterial composites such as changing the encapsulating polymer and using a different silver halide nanoparticle (AgCl and AgI) are being carried out.

Experimental Section

Materials and Instrumentation. Poly(vinylpyridine) (MW, 60 000), silver *para*-toluenesulfonate (99+%), and sodium *para*-toluenesulfonate were purchased from Aldrich. 1-Bromohexane (99+%), methanol, nitromethane, and dimethyl sulfoxide (all ACS grade) were purchased from Acros Organics. Bacterial growth media and agar were purchased from Difco. ^{1}H and ^{13}C NMR spectra were recorded on a Brucker DPX-300 instrument. A Reichart-Jung Ultracut E Microtome was used for sectioning the composite samples for TEM imaging. TEM imaging and X-ray microanalysis were done on a JEOL JEM 1200EXII electron microscope equipped with an energy-dispersive X-ray system operating at an accelerating voltage of 80 kV. X-ray diffraction spectra were recorded on a Philips X'Pert-MPD diffractometer using mono-

(38) (a) La Motta, E. J.; Hickey, R. F.; Buydos, J. F. *J. Environ. Eng. Div. (Am. Soc. Civ. Eng.)* **1982**, *108 (EE6)*, 1326−1341. (b) Beech, I. B.; Gubner, R.; Zinkevich, V.; Hanjangsit, L.; Avci, R. *Biofouling* **2000**, *16*, 93−104.

chromatized Cu Kα (λ = 1.5418 Å) radiation. Thermogravimetric analysis was performed on a TA Instruments TA250 F unit under a 100 mL/min argon flow. A JEOL JSM5400 scanning electron microscope operating at 10 kV in high vacuum mode was used for obtaining the biofilm images.

Synthesis of NPVP Polymer. The 43% **NPVP** was synthesized by heating poly(vinylpyridine) (1.5 g, 0.014 mol) in 25 mL of nitromethane with 0.5 equiv of 1-bromohexane (1.17 g, 0.007 mol) at 60 °C for 24 h. The polymer was isolated by precipitation in diethyl ether and dried under vacuum for 24 h. Yield: 2.4 g, 90%. A similar procedure was followed to synthesize the 21% **NPVP**. The degree of N-alkylation was determined by ^{1}H NMR peak ratios. ^{1}H NMR (300 MHz, DMSO-d_6, ppm): 8.95 (br, 2H), 8.26 (br, 2H), 7.66 (br, 2H), 6.70 (br, 2H), 4.54 (br, 2H), 2.2−1.17 (br, 11H), 0.89 (br, 3H). ^{13}C NMR (75 MHz, DMSO-d_6, ppm): 150.34, 145.25, 127.76, 123.87, 60.68, 42.76, 35.63, 31.48, 26.04, 22.77, 14.74.

Synthesis of AgBr/NPVP Polymer Composites. To prepare the AgBr-containing composites, **NPVP** (0.5 g) was dissolved in 5 mL of dry nitromethane. The required amount of AgPTS was dissolved in 5 mL of a 1:1 (v/v) mixture of dimethyl sulfoxide/nitromethane. Both the polymer and the AgPTS solutions were cooled to 0 °C in an ice bath. AgPTS solution was then added dropwise to the stirring polymer solution over a time period of 15 min. The mixture was stirred for another 30 min at room temperature. The polymeric composite was precipitated in diethyl ether and was dried under vacuum for 24 h to yield a yellow solid. This solid was then redissolved in methanol, and the resultant solution was used to cast composite films for antibacterial testing. For TEM imaging, pieces of solid polymer monoliths were sectioned into thin slices using the ultracut microtome. XRD diffraction patterns were obtained on finely ground solid composite samples placed on a glass holder.

Atomic Emission Spectrometry. Ag^+ ion concentration in broth was measured using a Leeman Labs RS 3000UV inductively coupled plasma emission spectrophotometer (Argon Plasma, Ag 328.068-nm excitation, Ag sensitivity of 0.005 ppm). The 1:2 AgBr/21% **NPVP** (0.425 g, containing 0.080 g of AgBr) and 1:1 AgBr/21% **NPVP** (0.279 g, containing 0.079 g AgBr) were taken in 50-mL Corning polypropylene tubes. The required amount of LB broth was added to each tube such that the ratio between volume (mL) of the LB broth and the weight (g) of AgBr present in the composites was kept constant at 100:1 (8.00 mL for 1:2 AgBr/21% **NPVP** and 7.90 mL for 1:1 AgBr/21% **NPVP**). The tubes were then incubated at 37 °C in a shaker operating at 250 rpm. After 24 h, the suspension was filtered through a 0.2-μm filter to remove solid insolubles, and the concentration of soluble Ag^+ ions in broth was measured using the emission spectrophotometer. The observed concentration of Ag^+ in ppm was divided by the weight of AgBr present in the composite to get ppm of Ag^+ generated per gram of AgBr present. This was repeated two more times for each composite, and the average of three measurements is reported.

Antibacterial Testing. Biosafety. Bacteria are potentially hazardous (especially methicillan-resistant *S. aureus*), and care should be taken while working with them. Standard biosafety lab techniques were followed while handling bacteria, human mammalian fluids, and various media. Gloves were used during all experimentation, and any accidental spills were immediately sterilized using 70% ethanol/water followed by bleach. The work area was also sterilized with 70% ethanol/water after completion of work. Unused media and bacterial suspensions were first deactivated with commercial bleach for 1 h before being disposed in biosafety bags. All material that had come in contact with bacteria (e.g., pipet tips, tubes, agar plates, etc.) was also thrown in biosafety bags in tightly closed bins. Biosafety bags were autoclaved for 2 h before final disposal.

Bacterial Culture. *E. coli* DH5-α (Clontech) was grown at 37 °C and maintained on LB plates (Luria-Bertani broth, Lennox modification, with 1.5% agar). *B. cereus* UW85 (ATCC 53522, a kind gift of Dr. J. Handelsman) was grown at 30 °C and maintained on LB plates. methicillan-resistant *S. aureus* (ATCC BAA-811) and *P. aeruginosa* wild-type strain PAO1 were grown in LB broth at 37 °C for 18−20 h from previously frozen inoculums.[39c] The relationship between absorbance at 590 nm (OD_{590}) and colony-forming units per milliliter was determined using the plate count method as described by Herigstad et al.[39b] This allowed the standardization of assay inoculums by measurements of OD_{590}. Bacteria were cultured for 16−18 h in LB broth, and cell counts were quantified by OD_{590} measurement. The cultures were then diluted to the appropriate density in LB broth.

Kirby Bauer Testing. A modified Kirby Bauer disk diffusion method was used to study the antibacterial activity of the composites.[22a] Square pieces of Whatman filter paper were coated with respective composites and control solutions by placing 3 × 50 μL of a 5% w/v solution in methanol on the paper and allowing the solvent to evaporate. Freshly grown bacteria were diluted by LB broth to yield stock solutions having approximate concentrations of 5×10^7 and 7×10^7 cfu/mL for *E. coli* and *B. cereus*, respectively. A quantity of 100 μL of this stock solution was plated on LB agar growth plates (1% agar). The composite and control-coated papers were placed on top of the inoculated agar plates and incubated overnight at 37 °C for *E. coli* and 30 °C for *B. cereus*. Colonies were visualized the next day, and digital images of the plates were captured. Image J 1.34n, free software available by NIH, was used to measure the zone of inhibition in digital pictures of the plates. A vernier caliper with an error of 0.1 mm was used for measurements.

Airborne Bacteria Testing. For surface testing of composite coating on glass, 150 μL of a 5 wt % composite solution in methanol was coated on a glass slide. A saturated suspension of *E. coli* was centrifuged at 4000 rpm for 5 min. The cells were resuspended in Nanopure water to yield a concentration of 10^6 cfu/mL. A sterilized chromatography sprayer (General Glassblowing, Richmond, CA) was used to spray a fine mist of the above cell suspension onto the slides, which were then placed into empty polystyrene Petri dishes (VWR, 100 × 15 mm) and air-dried for 5 min. Autoclaved LB broth (with 1% agar) that had been allowed to cool to approximately 40 °C was added to the bacteria-exposed slides. After the agar had solidified, the slides were incubated at 37 °C for 18 h and colonies were quantified.

Minimum Inhibitory Concentration Testing. Water-insoluble compounds were assayed in a modified macrodilution broth format.[33] Compounds (∼2−10 mg) were added to sterile polypropylene tubes, 14 mL (Falcon) or 50 mL (Corning), and the appropriate volume of a solution containing approximately 5×10^5 cfu/mL of *E. coli* or *B. cereus* in LB broth was added. Compounds were tested in triplicate at final concentrations of 50, 100, 250, 500, 1000, and 10 000 μg/mL. Negative control tubes contained only inoculated broth. The tubes were incubated at 37 °C (*E. coli*) or 30 °C (*B. cereus*) with shaking at 250 rpm for 18−20 h. The visual turbidity of the tubes was noted both before and after incubation. Aliquots from tubes (100 μL) that appeared to have little or no cell growth were plated on LB agar plates to distinguish between bacteriostatic or bactericidal effects. These were incubated at 37 °C (*E. coli*) or 30 °C (*B. cereus*) for 16−20 h, and then colonies were quantified.

Extended Antibacterial Testing. Required amounts of solid samples (∼2 mg) were added to sterile polypropylene tubes, 14 mL (Falcon). A quantity of 4 mL of a solution containing approximately 5×10^5 cfu/mL of *E. coli* or *B. cereus* in LB broth was added, and the tubes were incubated for 18−20 h at 37 °C (*E. coli*) or 30 °C (*B. cereus*) with shaking at 250 rpm. Turbidity was visually noted after incubation was complete. Aliquots of tubes (100 μL) that appeared to have little or no cell growth (LB broth clear) were plated on LB plates. The plates were incubated at 37 °C (*E. coli*) or 30 °C (*B. cereus*), and then colonies

(39) (a) *NCCLS Approved Standard*, 6th ed.; NCCLS: Villanova, PA, 2003; M7-A6. (b) Herigstad, B.; Hamilton, M.; Heersink, J. *J. Microbiol. Methods* **2001**, *44*, 121−129. (c) Kiriukhin, M. Y.; Debabov, D. V.; Shinabarger, D. L.; Neuhaus, F. C. *J. Bacteriol.* **2001**, *183*, 3506−3514.

were quantified. The tubes were then centrifuged at 400 rpm for 3 min to settle any possible piece of floating composite. The old LB was then carefully decanted (composites and polymers were insoluble and remained behind), and fresh bacterial suspension in LB (4 mL of 5×10^5 cfu/mL of *E. coli* or *B. cereus*) was added. The cycle was then repeated as described above for 17 days.

Bactericidal Kinetics Testing. Measured amounts of solid samples were added to sterile polypropylene tubes, 14 mL (Falcon). A quantity of 4 mL of a solution containing approximately 5×10^5 cfu/mL of *E. coli* in LB broth was added, and the tubes were kept in an incubated shaker at 37 °C. The initial time of addition of the LB−*E. coli* broth to the tubes was taken as zero, and 10 μL aliquots were withdrawn from each of the tubes at set time intervals. These aliquots were added immediately to 990 μL of LB broth that had been maintained at 4 °C to arrest further bacterial cell division. This solution was further diluted by a factor of 10, and 100 μL of the final solution was plated on LB agar plates. The plates were incubated at 37 °C for 18−20 h, and bacterial colonies were counted. A plot of cfu versus time was then plotted (Figure 7).

Mammalian Systems. MEM was purchased from GIBCO. Human serum was purchased from Sera Care Life Science, Inc. Blood (EDTA anticoagulant) and saliva were provided by human donors. Different weights of composites and polymers (0.4−2 mg) corresponding to MIC values of 50−10 000 μg/mL were added to sterile polypropylene tubes, 14 mL (Falcon). Respective mammalian fluid (0.5 mL) (serum, saliva, or blood) sufficient to cover the composites was added to each tube and incubated at room temperature in a shaker at 500 rpm for 5 h. Then 4 mL of suspension of *S. aureus* (5×10^5 cfu/mL) in MEM containing 30% human serum was added, and tubes were incubated at 37 °C in a shaker at 250 rpm for 18 h. Aliquots of 100 μL were plated on LB agar plates and incubated at 37 °C for 16−20 h, and colonies were counted.

Biofilm Formation. Glass surfaces ($\sim 1 \times 1$ cm) were coated with 3×150 μL of a 5 wt % of 1:1 AgBr/21% **NPVP** composite or 21% **NPVP** solution in methanol. *P. aeruginosa* was cultivated at 37 °C for 20 h in LB broth. It was then diluted with LB to yield a final concentration of 1×10^7 cfu/mL. A quantity of 5 mL of this bacterial suspension was transferred to sterile polypropylene tubes. Coated glass pieces were then placed in these tubes for biofilm formation and were incubated at 37 °C in a shaker at 250 rpm. Old media was decanted, and 5 mL of fresh LB was added after every 24 h. Coated pieces were removed after 24, 48, and 72 h. The pieces were gently rinsed by dipping 3 times in phosphate-buffered saline (pH 7.4) and were placed in a fixative (1% v/v glutaraldehyde and 4% v/v formaldehyde) overnight. The pieces were then rinsed 3 times with 0.1 M phosphate buffer and were then dehydrated in a series of acetone washes (25% for 5 min, 50% for 5 min, 75% for 5 min, 90% for 5 min, and 100% for 2×5 min). Finally the samples were dried by CO_2 critical point (BAL-TEC CPD 030 Critical Point Drier), mounted on aluminum stubs, coated with gold/palladium, and imaged in high vacuum mode at 10 kV.

Acknowledgment. This work was supported by the Huck Institute of the Life Sciences and the Materials Research Institute of The Pennsylvania State University. We thank Missy Hazen of the Electron Microscopy Facility of the Huck Institute for TEM imaging. B.R.P. thanks the NIH for financial support.

JA061442Z